Article

Simultaneous recording of the uptake and conversion of glucose and choline in tumors by deuterium metabolic imaging (DMI)

Andor Veltien[1], Jack van Asten[1], Niveditha Ravichandran[1], Robin A. de Graaf [2], Henk M. De Feyter[2], Egbert Oosterwijk[3], Arend Heerschap[1*]

[1] Department of Medical Imaging (Radiology), Radboud University Medical Centre, Nijmegen, The Netherlands
Andor.veltien@radboudumc.nl ; sjaak.vanasten@radboudumc.nl ; n.ravichandran@science.ru.nl; arend.heerschap@radboudumc.nl ;

[2] Department of Radiology and biomedical imaging, Yale University, New Haven, CT, United States
Robin.degraaf@yale.edu ; henk.defeyter@yale.edu

[3] Department of Urology, Radboud University Medical Centre, Nijmegen, The Netherlands
Egbert.oosterwijk@radboudumc.nl

***) Corresponding author:**
Arend Heerschap, PhD
Department of Medical Imaging (Radiology), 767
Radboud University Medical Centre
PO Box 9101
NL-6500 HB Nijmegen, the Netherlands
+31 24 3614795
arend.heerschap@radboudumc.nl

Running title: DMI of choline simultaneous with glucose

Simple summary: Tumors increase their glucose and choline uptake to support growth. These properties are employed to detect and identify tumors in the body by imaging the uptake of radio-isotope analogs of these compounds. In this study we show that deuterium metabolic imaging (DMI), a new MRI method to image metabolites using non-radioactive labeling with deuterium, can image choline uptake in tumors. Furthermore, we demonstrate that DMI can image the tumor uptake of choline and of glucose, and additionally its metabolic conversion, simultaneously, in contrast to radio-isotope imaging that only assesses the uptake of one radio-isotope labeled compound at a time. For these reasons and also because DMI is relatively simple and can be combined with other MR methods it is a promising modality for a more specific tumor characterization than by separate imaging of the uptake of radio-isotope labeled glucose or choline.

Abstract: Increased glucose and choline uptake are hallmarks of cancer. We investigated if the uptake and conversion of [$^2H_9$]choline alone and together with that of [6,6' $^2H_2$]glucose can be assessed in subcutaneous tumors by deuterium metabolic imaging (DMI) after bolus administration of these compounds. Therefore tumors with human renal carcinoma cells were grown subcutaneously in mice up to ~0.5 cm^3. Mice were anesthetized with isoflurane and IV infused in the MR magnet for ~20 sec with ~0.2 ml solutions containing either [$^2H_9$]choline (0.05g/kg) alone or together with [6,6' $^2H_2$]glucose (1.3g/kg). ^2H MR was performed on a 11.7T MR system with a home-built $^2H/^1H$ coil using a 90^0 excitation pulse and 400ms repetition time. 3D DMI was recorded at high resolution (2x2x2mm) in 37 min or at low resolution (3.7x3.7x3.7mm) in 2:24 min. Absolute tissue concentrations were calculate assuming initial [HOD]=13.7mM. Within 5 minutes after [$^2H_9$]choline infusion its signal appeared in tumor spectra representing concentration increasing up to 0.3–1.2 mM and then slowly decreased or remained constant over 100 minutes. In plasma [$^2H_9$]choline disappeared within 15 minutes post-infusion implying that its tumor signal arises from tissue and not blood. After infusing a mixture of [$^2H_9$]choline and [6,6' $^2H_2$]glucose their signals were observed separately in tumor ^2H spectra. Over time the [$^2H_9$]choline signal broadened, possibly due to conversion to other choline compounds, [[6,6' $^2H_2$]glucose] declined, [HOD] increased and a lactate signal appeared, reflecting glycolysis. Metabolic maps of all ^2H compounds were reconstructed from high resolution DMIs. As choline infusion and glucose DMI is feasible in patients, their simultaneous detection has clinical potential for tumor characterization.

Keywords: MRI, deuterium metabolic imaging, tumor, ^2H, glucose, choline

A preliminary version of this work has been presented at the virtual European Molecular Imaging Meeting 24-28 august 2020

1. Introduction

Enhanced glucose uptake is a hallmark of malignant tumors. For diagnostic purposes this is traditionally assessed by PET using the glucose analog ^{18}Fluordeoxyglucose (FDG) [1]. However, this method cannot monitor subsequent glucose catabolism. For in vivo applications ^{13}C MR spectroscopy has been used to probe uptake and metabolic conversions of non-radioactive ^{13}C labeled glucose in tumors into lactate and other compounds [2, 3]. The low SNR of the method precluded to employ it as an imaging method although recently reported denoising methods may favor better imaging conditions [4]. Hyperpolarisation of ^{13}C nuclei in labeled compounds considerably improves the SNR of their signals. Applying these compounds to the body enables imaging of metabolic processes otherwise not detectable by MR, but this method is limited by a short time window of visibility, in particular for glucose due to short T1 relaxation times of the ^{13}C nuclei in this molecule [5, 6]. A further possibility for enhanced glucose detection in MR is provided by chemical exchange saturation transfer (CEST) imaging by which proton exchange between water and glucose is employed to exploit the large magnetic pool of water protons for an SNR increase in the detection of the glucose moiety. However, the method may be rather non-specific due to various interactions in which these protons are involved and it also gives no direct view on glucose catabolism [7].
Recently deuterium (^{2}H or D) MR to trace deuterated metabolites in the body, after administration of deuterated substrates, has gained new momentum under the names of deuterium metabolic spectroscopy (DMS) or imaging (DMI), in particular for the spatial monitoring of glucose uptake and its conversion in the brain and brain tumors using non-radioactive [6,6' $^2H_2$]glucose as substrate [8-10]. DMI has several advantages, e.g. by tracking ^{2}H in lactate and combined glutamine and glutamate signals it provides a quantitative biomarker for the Warburg effect [9] and for the glycolytic pathway in tumors [11]. A potential clinical advantage of the method is the simplicity of its application compared to FDG-PET and hyperpolarization MR [9].
Enhanced choline uptake is another hallmark of cancer and the uptake of choline compounds in tumors has been assessed by ^{18}F or ^{11}C choline PET for diagnostic purposes [12]. Often choline-PET identifies tumors better than FDG-PET [13, 14]. Increased steady state levels of choline compounds in tumors can be mapped by ^{1}H MR spectroscopic imaging, but separation of its different species is not possible [12, 15]. The main different phosphorylated choline compounds can be detected by ^{31}P MR spectroscopic imaging employing ^{1}H decoupling or high magnetic fields (≥ 7T), although at a lower spatial resolution than total choline detection by ^{1}H MR spectroscopic imaging [16] [12, 17]. It is possible to obtain choline in which the 9 protons at the methyl groups are replaced by deuterons which is favorable for a good SNR in DMI.
The aims of this study were to demonstrate the feasibility of DMI to monitor [$^2H_9$]choline uptake in subcutaneous tumor models and of simultaneous recording of the uptake and conversion of glucose and of choline in these tumors by DMI.

2. Materials and Methods

Tumors and animal handling

Animal experiments were conducted according to institutional guidelines and regulations and were approved by the national Central Animal Experiments Committee (CCD) and the local animal welfare body (RU-DEC-2017-0038-12 and RU-DEC-2017-0038-013). Mice (age 6-8 weeks) were kept under specified pathogen free conditions and received food and water ad libitum. Human renal carcinoma cells were subcutaneously injected in the flank of athymic female BALB/c nu/nu mice (SKR17T-CA9-Luc cells) or of NSG (NOD SCID) mice (NU12 cells) and tumors were grown up to about 0.5 cm^3 in size. Before the MR experiments they were anesthetized by applying 1 – 2 % isoflurane in a mixture of O_2/N_2O = 2:3 through a mask. Respiration rate was maintained at 60-80 bpm. Body temperature was monitored with a rectal probe and maintained at about 37^{0}C with heated air. A catheter was placed in a tail vein for infusion of solutions with ^{2}H compounds. About 30 min before the MR measurement mice were IM injected with 12 µg atropine to prevent a possible cholinergic reaction of the choline bolus. At the time of the MR experiments the animals weighted 24 - 38 g.

MR hardware and IV infusions

Mice were placed prone in the small bore magnet of an 11.7T BioSpec Avance III animal MR system (Bruker BioSpin GmbH, Ettlingen, Germany). The tumors were positioned inside a circular ^{2}H coil with 16 mm diameter (76.8MHz) which was surrounded by a circular ^{1}H coil of 25 mm diameter (500.3MHz).
Inside the magnet the mice were IV infused with a saline solution of ~ 0.2 ml in ~20 sec containing either 0.05g/kg [$^2H_9$]choline or 0.05g/kg [$^2H_9$]choline combined with 1.3g/kg [6,6 $^2H_2$]glucose. The ^{2}H compounds were obtained from Sigma-Aldrich.

Deuterium MR spectroscopy and imaging

First T_2 weighted RARE ^{1}H MR images were recorded with the ^{1}H coil to check the proper positioning of the tumors in the ^{2}H coil (echo time (TE): 30 ms, repetition time (TR): 2500 ms, field of view (FOV): 20x20 mm, matrix 128×128 and a slice thickness (ST) of 1 mm) and T_1 weighted 3D FLASH ^{1}H MR images (TE: 2.3 ms; TR: 20 ms; flip angle : 10^0, FOV:

Preprints (www.preprints.org) | NOT PEER-REVIEWED | Posted: 8 July 2021 doi:10.20944/preprints202107.0189.v1

33x33x33 mm; matrix63x63x63) were acquired as reference images for the DMI. Guided by the anatomical images a volume of interest (VOI) of variable size (e.g. 5x3x5 mm) was selected inside the tumor to optimize magnetic field homogeneity on the line width of the water signal using a PRESS sequence.
Deuterium MR spectra (DMS) were recorded with a pulse-acquire sequence using a 50 µs square excitation pulse of about 90^0 in the center of the coil. The pulse repetition time (TR) was 500 ms, the acquisition band width was 14 ppm and 300 averages were acquired in a total acquisition time of 2:24 min. 3D DMI was performed with a 1 ms composite RF pulse, optimized to provide circa five-fold immunity towards RF inhomogeneity over a spectral bandwidth > 600 Hz, with TR = 400 ms and TE = 0.4 ms either at a high spatial resolution with a FOV of 30x30x30 mm and matrix size 15x15x15 resulting in nominal voxels of 2x2x2 mm (8 µL) obtained in 37 min or at low spatial resolution with a FOV of 33x33x33 and matrix size 9x9x9 resulting in a nominal voxels of 3.7x3.7x3.7mm (~50 µL) recorded in 2:24 min. The k-space data were acquired with spherical sampling in 3D.

Data processing
Deuterium metabolic imaging data was handled in DMIWizard (Fourier transform, phasing, filtering, image reconstruction), a home-written Matlab-based graphical user interface for processing of 1D DMS and 3D DMI data. After FT of the time series of 45 FIDs the ^{2}H MR spectra were frequency aligned and to improve the SNR a moving average of 3 spectra was applied using jMRUI software [18]. Within jMRUI the program AMARES was used to fit the signals of water (HOD), choline (Cho), glucose (Glc) and lactate (Lac), assuming a Lorentzian line shape. The glucose signal was approximated with 2 Lorentzian shaped lines, resonating 4.6 Hz apart. As additional prior knowledge in the fitting the relative resonance frequencies of the signals were included relative to HOD at 4.8 ppm (Glc1 at 3.83 ppm, Glc2 at 3.77 ppm, Cho at 3.2 ppm and Lac at 1.3 ppm) and line widths were constrained between 10 and 60 Hz. Absolute tissue concentrations were determined using the initial HOD signal as an internal reference assuming a natural abundance HOD concentration of 13.7 mM [8]. Tissue concentrations of compounds were normalized with respect to the number of deuterons attached to them.

Blood samples
To determine ^{2}H labeled compounds in blood, samples of 0.5 ml were obtained from a puncture of the heart of the mice after infusion. Plasma was derived from the blood samples by centrifugation for 5 minutes at 5000 rpm to separate it from cells. ^{2}H NMR spectra of 200 µl plasma samples were recorded at 500 MHz on a Bruker AVANCE III vertical bore NMR system (Bruker BioSpin, Germany) at a bandwidth of 12 ppm with 5k data points and 512 acquisitions. The repetition time was 5 seconds. If needed measurements per time point were frequency aligned and averaged in jMRUI and for fitting AMARES was applied using the same prior knowledge as for the in vivo spectra.

3. Results

DMS and DMI of renal tumor after [$^2H_9$]choline infusion
To test if we could monitor the uptake of $^2H_9$ choline in a subcutaneous tumor we infused 0.05g/kg of a saline solution of about 0.15 ml of this compound for ~15 sec in the tail vein of a mice carrying an SKRC17T tumor. On a T2 weighted MR image recorded with the ^{1}H coil the tumor can be seen (Fig. 1A). In a volume of 7x6x7 mm in the tumor the magnetic field homogeneity was optimized to a water line width of 65 Hz. The ^{2}H MR spectrum recorded with the ^{2}H coil, without further localization, before the infusion only showed a signal for natural abundance HOD (Fig. 1B). Immediately after the infusion a ^{2}H signal appeared at ~3.2 ppm, well separated from that of HOD, which is assigned to the deuterated methyl groups of choline compounds. From its signal integral we deduced that its tissue concentration increased to a maximum level of ~1.2 mM [$^2H_9$]choline at ~5 min post-infusion and then declines to 0.9 mM at ~15 min post-infusion after which it slowly decreased to ~0.7 mM at 100 min post-infusion (Fig. 1D). Over this time period the HOD signal remained almost constant (Fig 1E) and no other resolved ^{2}H signals were observed. Shortly after the infusion the unfiltered line width of the unlocalized signal for HOD was about 38 Hz and for [$^2H_9$]choline about 25 Hz. In the 100 min thereafter the linewidth of HOD did not change, but that of [$^2H_9$]choline steadily increased to about 36 Hz (Fig. 1F). From a high resolution 3D DMI obtained between about 60 and 90 min post-infusion a [$^2H_9$]choline map could be reconstructed (Fig. 1C).

Preprints (www.preprints.org) | NOT PEER-REVIEWED | Posted: 8 July 2021 doi:10.20944/preprints202107.0189.v1

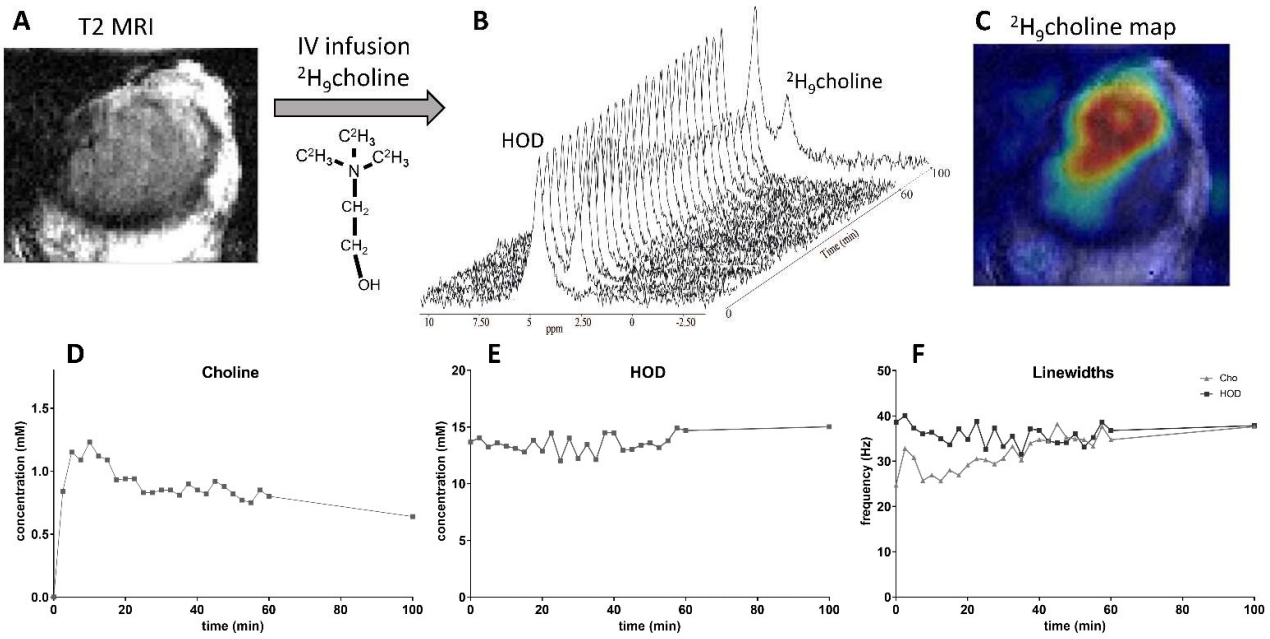

Figure 1. Deuterium MR of a human renal tumor (SKRC17T) subcutaneously grown in a BALB/c mice.

A. T2 MRI of the tumor. The chemical structure of [$^2H_9$]choline is also indicated.

B. Unlocalized ^2H MR spectra obtained with a surface coil at a time resolution of 2:30 min. The first spectrum recorded before the infusion of choline only shows a natural abundance HOD signal at 4.8 ppm. Immediately after the infusion of a bolus of about 0.2 ml with [$^2H_9$]choline a signal for this compound is observed at about 3.2 ppm. Within ~5 min after the infusion this signal has reached its maximum value and then slowly declines over time.

C. A metabolic map of [$^2H_9$]choline reconstructed from a high resolution DMI obtained between 60 and 100 min post-infusion.

D. [$^2H_9$]choline tissue concentration (mM) as a function of time post-infusion. After a rapid initial increase it slowly decreases over time.

E. HOD tissue concentration (mM) as a function of time. Over the measurement period of 100 min the HOD concentration essentially remains constant.

F. Fitted linewidths (Hz) of the [$^2H_9$]choline and HOD resonances as a function of time. That of HOD essentially remains constant, while that of [$^2H_9$]choline increases.

To test how well the ^2H signals of [$^2H^9$]choline and of [6,6' $^2H_2$]glucose are separated we recorded ^2H MR spectra of a phantom containing 2 tubes, one filled with [$^2H_9$]choline and the other with [6,6' $^2H_2$]glucose. An unlocalized ^2H MR spectrum of the phantom showed that the ^2H signals of choline and glucose are well-resolved (Fig. 2A). Using a single Lorentzian line to fit these resonances resulted in a line width of 17.1±4.2.Hz (SD of fit error) for choline and 32.2±4.3 Hz for glucose. The measurement of a 3D high resolution DMI of the phantom enabled the reconstruction of separate maps for glucose (Fig 2B) and choline (Fig. 2C) in the tubes.

Subsequently we investigated if it was also possible to observe separated choline and glucose signals in ^2H spectra of a subcutaneous tumor by performing a 20 sec infusion of a solution with [$^2H_9$]choline and [6,6' $^2H_2$]glucose in the tail vein of an NSG mouse carrying a NU12-Luc-GFP tumor (Fig. 2D) and recording a high resolution 3D DMI. In a ^2H MR spectra of an 8 µl voxel in the DMI of the tumor the deuterated choline and glucose signals are well separated and also a resolved signal for deuterated lactate is observed (Fig. 2E). The tissue concentration of [$^2H_9$]choline averaged over the time of the DMI recording of 37 min, was about 2 mM and its line width was 19 Hz. For each of the deuterated compounds with signals in the ^2H MR spectra we reconstructed metabolic maps parallel to the circular RF coil: HOD (Fig 2F), glucose (Fig 2G), choline (Fig 2H), and lactate (Fig 2I). Although signal distribution in these maps is

 doi:10.20944/preprints202107.0189.v1

also determined by the sensitive field of the RF coil a comparison of the signal intensities in the maps of the metabolites, which is expected to be the same if only determined by the RF field, indicate differences in their distributions.

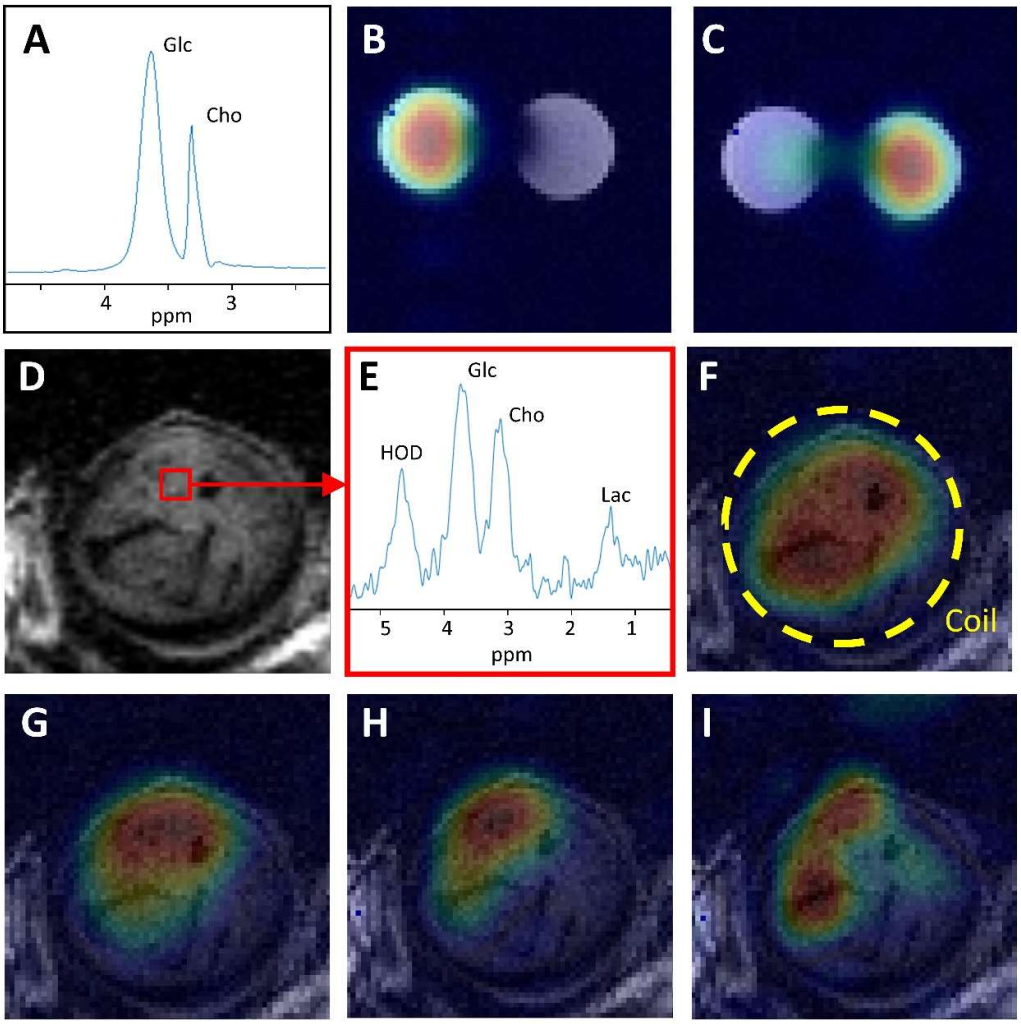

Figure 2. Deuterium metabolic imaging study of deuterated glucose and choline in phantom and in human renal tumor subcutaneously growing in mice.

A. An unlocalized ^{2}H MR spectrum of 2 tubes, one filled with a saline solution of $^{2}H_9$ choline (63 mM) and the other with a saline solution of [6,6'-$^{2}H_2$]glucose (0.71 M). The glucose signal is completely separated from the choline signal.

B. [6.6'-$^{2}H_2$]glucose map reconstructed from high resolution DMI of both tubes

C. [$^{2}H_9$]choline map reconstructed from high resolution DMI of both tubes

D. T2 weighted MR image of a slice through a NU12 renal carcinoma growing in the flank of an NSG mice. A voxel of 8 µl is indicated which was selected from a high resolution 3D DMI recorded in 37 min after IV application of a mixture of [6,6'-$^{2}H_2$]glucose and [$^{2}H_9$]choline.

E. The ^{2}H MR spectrum of the 8 µl voxel selected from the tumor shows signals for water (HOD), glucose (Glc), choline (Cho) and lactate (Lac). The spectrum was filtered with a 2Hz exponential line broadening. The glucose and choline signals are clearly separated.

F. HOD map reconstructed from 3D DMI

 doi:10.20944/preprints202107.0189.v1

G. Glucose map reconstructed from 3D DMI

H. Choline map reconstructed from 3D DMI

I. Lactate map reconstructed from 3D DMI

The maps are oriented parallel to the ^{2}H RF coil (indicated by a circle in F) and projected on top of T1 MR images.

To examine if we can follow the conversion of [6,6' $^{2}H_2$]glucose into lactate over time in the presence of [$^{2}H_9$]choline in a tumor we recorded sequential low spatial resolution DMIs at a time resolution of 2:24 min after the infusion of a mixture of these compounds into mice carrying a subcutaneous SKRC 17-CA9-Luc tumor (Fig 3A). A stack plot of ^{2}H MR spectra and the calculated tissue concentrations of compounds in these spectra as a function of time are displayed in Fig 3B and C-F. The HOD level is steadily increasing over time (Fig. 3C), while the glucose content is increasing to a maximum concentration of about 8 mM in 5 – 10 min and then declines (Fig. 3D). During this decline a signal at 1.3 ppm for lactate appeared (Fig. 3E). The [$^{2}H_9$]choline tissue concentration increased to values between 0.3 and 0.4 mM and remained stable up to 100 min. The line width of the [$^{2}H_9$]choline signal increased from about 10 Hz immediately after infusion to about 15 Hz after 100 min.
Similar results were obtained in two other mice carrying tumors of the same batch. For all 3 tumors the average tumor tissue concentration between 20 and 60 min post-infusion for [$^{2}H_9$]choline was 0.32 ± 0.05 mM and for deuterated lactate 0.86 ± 0.27 mM. The maximum average [6,6' $^{2}H_2$]glucose tissue concentration at 10 min post-infusion was 8.87 ± 2.58 mM. Initial linewidths of compound signals in the spectra of all tumor DMIs, recorded shortly after the infusion, depended on the magnetic field shimming results.

Preprints (www.preprints.org) | NOT PEER-REVIEWED | Posted: 8 July 2021 doi:10.20944/preprints202107.0189.v1

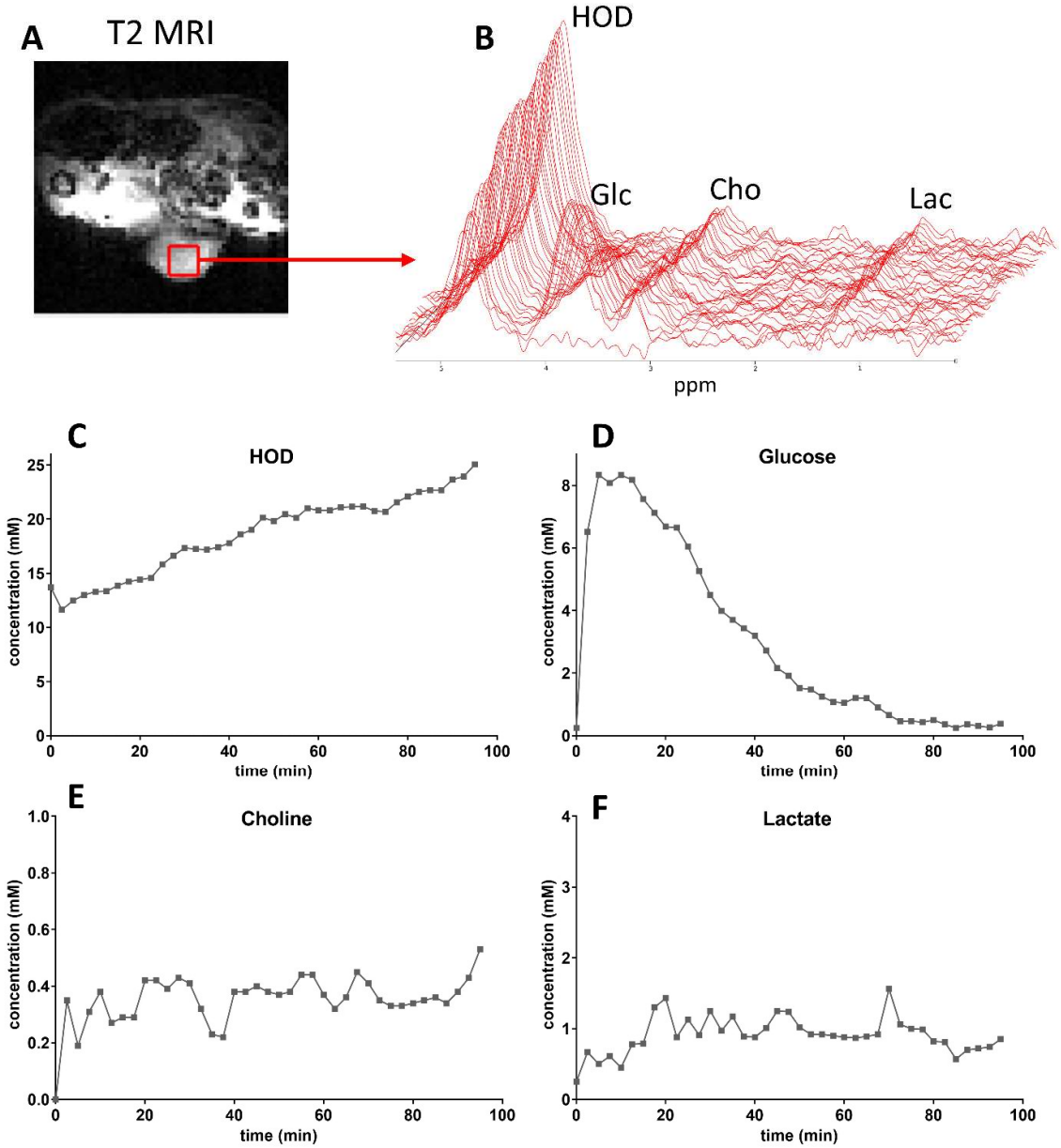

Figure 3. Low spatial resolution 3D DMI (50 µl voxels), recorded at a time resolution of 2:24 min, from an SKRC 17T-CA9-Luc tumor growing in the flank of a mice.

A. T2 weighted MRI with a selected voxel inside tumor indicated

B. Time series of ^{2}H MR spectra consecutively recorded from this voxel over a period of 90 min showing an increasing HOD signal, an increasing and decreasing glucose signal, a rapidly increasing and then constant choline signal and a signal for lactate appearing during the decline of the glucose signal.

C - D. Time curves of metabolite tissue concentrations (mM)

In ^{2}H NMR spectra of blood plasma taken immediately after infusion of a mixture of [6,6' $^{2}H_2$]glucose and [$^{2}H_9$]choline, ^{2}H signals of both compounds can be detected next to that of HOD (Fig 4A). Their concentrations were estimated to be 2.6 mM for choline and 11.6 mM for glucose. From spectra taken at 15 min or longer after infusion

Preprints (www.preprints.org) | NOT PEER-REVIEWED | Posted: 8 July 2021 doi:10.20944/preprints202107.0189.v1

no choline signal could be detected and the glucose signal was strongly decreased (Fig 4B). No significant signal for [$^2H_9$]betaine, the first breakdown product of choline at about 3.4 ppm was detected.

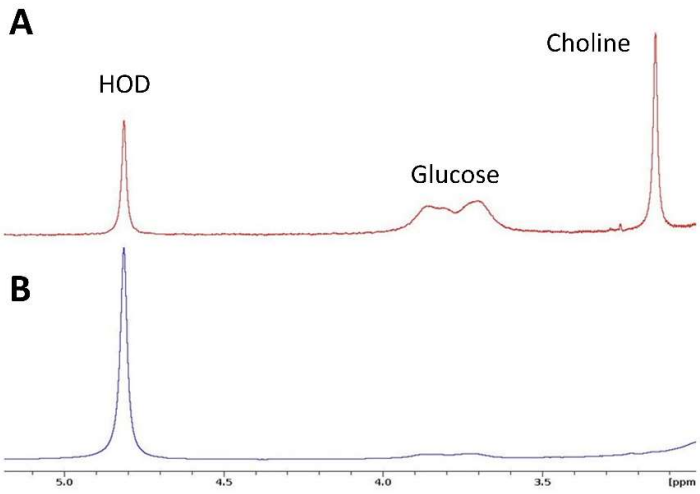

Figure 4. ^2H MR spectra recorded from plasma samples after infusion of a mixture of [6,6'-$^2H_2$]glucose and [$^2H_9$]choline in mice carrying a subcutaneous renal tumor.
A) Spectrum taken immediately after infusion

B) Spectrum taken 15 min after infusion. The ^2H signal for glucose is strongly reduced and that for choline signal is absent. Vertical scales are arbitrary.

4. Discussion

In this study we developed a protocol to follow the uptake and to image the presence of [$^2H_9$]choline in subcutaneous tumors growing in the flank of mice by ^2H MR spectroscopy (DMS) and imaging (DMI) after an IV bolus administration of this compound. In addition we were able to monitor simultaneously the uptake of [$^2H_9$]choline and of [6,6' $^2H_2$]glucose, and to follow its conversion into lactate, in subcutaneous tumors by DMI after an IV bolus administration of a mixture of both compounds . ^2H NMR spectra obtained of blood plasma at 15 minutes post-infusion showed that no ^2H labeled choline was present anymore in agreement with the short half-life of plasma choline of less than 1 minute in mice[19]. This implies that the [$^2H_9$]choline signal seen in the in vivo ^2H MR spectra arises from tumor tissue.
The maximum of the [6,6' $^2H_2$]glucose tissue concentration and its timing as recorded in the SKRC 17-CA9-Luc tumors, in which both [6,6' $^2H_2$]glucose and [$^2H_9$]choline was infused, is comparable to that in subcutaneously growing EL4 tumors recorded under similar infusion conditions and taking the specific normalization with the initial HOD concentration into account [11]. However, the deuterated lactate concentration in our tumors was much lower, which indicates an as yet unidentified difference in lactate metabolism.
The uptake of [$^2H_9$]choline in a subcutaneous tumor (an MCF7 human breast cancer model growing in CD1 athymic mice) has been previously monitored by ^2H MR spectroscopy at 4.7T using ISIS localization of a single voxel of 1cm^3 during continuous infusion at a low dose (16 µmol/kg/min) [20]. In contrast to our study the ^2H choline signal only appeared at about 40 min post-infusion, but then increased to a tissue concentration of about 1.5 mM, calculated assuming the HOD signal to be 16.4 mM, which is in the same order of the concentrations observed in the renal subcutaneous tumors (0.3 – 2 mM). During the infusion the plasma level of deuterated choline in the CD1 mice reached a constant level of 222± 22 µM while this choline concentration in plasma of our mice was estimated to be 2.6 mM immediately after the bolus. The $^2H_9$ choline signals in our tumor spectra were completely resolved from the HOD signal while this was only partly so in this study. Obviously the higher employed field strength contributed to a better resolution, but also the much smaller selected volumes of 50 µl and 8 µl and possibly the tissue composition of the tumor may have favored a better field homogeneity and improved spectral resolution.
The line width at FWHM of in vivo ^2H compounds is almost constant between 4 and 7T [21]. In our study the line width for the HOD signal from a DMI localized volume in the tumor varied between about 15 Hz and 25 Hz. This is larger than that reported for

Preprints (www.preprints.org) | NOT PEER-REVIEWED | Posted: 8 July 2021 doi:10.20944/preprints202107.0189.v1

the human brain at 4 and 7T [21], which is likely due to more difficult magnetic field shimming conditions as the line widths correlated with the shimming results. For choline we find line widths between about 10 and 20 Hz. As the spectral separation between these signals is ~1.5 ppm which translates to a separation of ~30 Hz at 3 T it follows that choline and HOD can also be separately observed at the clinical field strength of 3T assuming constant line widths. The separation between glucose and choline is about 0.5 ppm which translates to a separation of about 23Hz at 7T which will enable the separation of the signals of these compounds. At 3T with a separation of about 10 Hz only the smallest observed line widths of <15 Hz for the choline signal will allow acceptable separation of [$^2H_9$]choline and [6,6' $^2H_2$]glucose signals. However, the glucose signal disappears within ~ 60 mins post-infusion when the choline signal intensity has not changed much yet.

During the 90 or 100 min of recording ^{2}H MR spectra after only [$^2H_9$]choline infusion the HOD signal did not change much as expected with little loss of deuterons from [$^2H_9$]choline or its downstream products during this time period that might get involved in exchange with water. With this protocol of bolus administration we also did not detect any signal for [$^2H_9$]betaine, the main breakdown product of choline compounds.[22]

In all experiments with [$^2H_9$]choline infusion its tumor signal rapidly increased to a maximum level within 5 min and then slowly decreased or remained stable up to 100 min post-infusion. As we cannot discriminate among the choline species that contribute to the [$^2H_9$]choline signal it is not clear if the composition of these species remains constant or changes over time. Recent studies of ^{2}H NMR spectra obtained from biopsies from brain tumors in the rat supplied with [$^2H_9$]choline, indicated that free choline is being converted into phosphocholine and glycerophosphocholine within the tumor, although substantial amounts of free choline still seem to be present at 36 min after the start of the infusion [23]. In this respect it is interesting that in our experiments the line width of the [$^2H_9$]choline signal increases over time, apparently because of the contribution of other choline compounds with a slightly different chemical shift.

In this study we applied 0.05g/kg [$^2H_9$]choline as an IV bolus in about 20 sec. As this may give an acute cholinergic reaction [24] we first applied atropine to the mice as a preventive measure. To avoid the application of atropine the amount of [$^2H_9$]choline can be decreased and/or the infusion time can be extended. As the choline signal, after its rapid initial increase, only changes very slowly an extension may be most effective in rodent examinations. In other supplementation studies, in particular in humans, choline is administered as a continuous infusion or orally [25] [26, 27].

Choline imaging with enhanced sensitivity has also been explored with hyperpolarization by dynamic nuclear polarization (DNP) of [1,1,2,2 $^2H_4$, 1-^{13}C] choline[28] and the in vivo detection of DNP hyperpolarized ^{15}N choline in the rat was demonstrated [29]. In these experiments also precautions had to be taken to avoid cholinergic reactions because a bolus infusion with a solution at a relatively high choline concentration (~90 mM) is still required. The intrinsic sensitivity of the MR experiments using hyperpolarization is much better than that of the ^{2}H MR experiments. Although no one-to-one comparisons have been made yet, we anticipate that this difference will be largely compensated by the much longer time available for data acquisition in ^{2}H MR experiments and the 9 deuterons in $^2H_9$ choline contributing to its signal. Apart from this sensitivity issue, ^{2}H MR experiments are less complicated to perform and easier to analyze than hyperpolarization MR experiments.

Increased steady state levels of choline compounds are a common finding in tumors and are associated with demands for enhanced phospholipid metabolism to support cellular membrane synthesis in oncogenesis and tumor progression. This property has been explored in ^{1}H MR spectroscopic imaging by using the (relative) intensity of the overlapping signals of all choline compounds together as a non-invasive diagnostic marker for several cancers such as in the brain, prostate and breast [12]. An increased total choline signal may serve to localize the tumor and its quantified intensity to determine tumor stage or aggressiveness [15]. In tumor therapies the total choline signal intensity may serve to evaluate the effect of (experimental) treatments [30, 31]. Using choline tracer imaging such as in ^{11}C choline PET or in [$^2H_9$]choline DMI provides a more dynamic view on choline uptake than the steady state levels of MRS detectable choline metabolites. Compared to [$^2H_9$]choline DMI the application of ^{1}H MRSI has the technical challenge that in the latter the total choline signal has to be separated from the background of other proton signals, in particular of water and lipids. Compared to ^{11}C choline PET the application of $^2H_9$ choline DMI has the advantage that no radioactivity is involved and that in principle the measurement can be easily integrated within a multi-parametric MRI examination. Moreover, ^{11}C choline PET imaging is hampered by the short half-life of the ^{11}C isotope.

In this feasibility study we noticed that tumors may accumulate different levels of [$^2H_9$]choline and with variable spatial distributions. In future studies this has to be correlated with molecular features of these tumors such as proliferation markers, glucose and choline transporters, and with tumor heterogeneity.

Choline PET is often used in the diagnosis of prostate cancer [32, 33], but is also employed to identify other cancers in the body [14]. Choline DMI maybe used as a non-radioactive alternative with the additional advantage that it can be combined with multi-parametric MRI. Currently, RF coils of sufficient quality for DMI at 7T to diagnose tumors in the brain have been presented that appear to offer a spatial resolution comparable to that of choline PET [9]. Recently, also deuterium body coils have been presented and shown to be able to record DMI's, such as after [6,6' $^2H_2$]glucose application [9] [34]. It remains to be seen what spatial resolution can be achieved to detect and characterize tumors in the body as compared to FDG and choline PET imaging. Signal denoising methods may be helpful as these recently have been demonstrated to substantially improve SNR for DMI at 3T [35].

Conclusion

In this study we have demonstrated that DMI of [$^2H_9$]choline uptake in tumors subcutaneously growing in the mice is feasible, next to its demonstrated feasibility to detect brain tumors in the rat [25]. Moreover, we show that the simultaneous monitoring of [$^2H_9$]choline and [6,6' $^2H_2$]glucose and its catabolic product lactate in tumors by DMI is possible. This enables to obtain information from two main tumor properties at the same time, enhanced glucose uptake and catabolism and choline uptake, and therefore is expected to provide a more specific metabolic characterization of tumor lesions, than obtained with a single tracer, single parameter approach such as with FDG or choline PET.

As DMI of glucose uptake and its metabolic conversions has been shown to be feasible in patients [2], the simultaneous performance of choline DMI next to that of glucose is a complementary extension with clinical potential. The application of other combinations of deuterated compounds in tumor studies are foreseeable, as long as their resonances are spectrally resolved, such as for instance choline with the conversion of fumarate into malate to assess tumor cell death after treatments [36] or an inert deuterated compound to assess tumor perfusion.

Author contributions: Conceptualization: AH, AV, and EO; methodology: AV, AH, JvA, EO, RdG, and HdF; resources: AH, HdF, RdG and EO; data collection: AV, JvA, AH, and NR.; data analysis and results interpretation: AH, AV, JvA and NR; writing—original draft preparation: AH and AV; writing—review and editing: all authors. All authors have read and agreed to the published version of the manuscript.

Institutional Review Board Statement: The study was conducted according to the guidelines of the Declaration of Helsinki, and approved by the Institutional Review Board (or Ethics Committee) of the University Nijmegen and performed according to Dutch laws (RU-DEC-2017-0038-12 and RU-DEC-2017-0038-013).

Data Availability Statement: Data of this study is available by the last author upon reasonable request

Acknowledgments: We thank Bianca Lemmers-van de Weem and Kitty Lemmens-Hermans for excellent biotechnical assistance during tumor implantation and animal maintenance, Jeanette Oosterwijk-Wakka for technical support and Xander Staal for help with the atropine application. This study is supported in part by NIH grant R01 EB025840

Conflict of interest: The authors declare that they have no conflict of interest. The funders had no role in the design of the study; in the collection, analyses, or interpretation of data; in the writing of the manuscript, or in the decision to publish the results.

References

1. Gambhir, S.S., *Molecular imaging of cancer with positron emission tomography.* Nat Rev Cancer, 2002. **2**(9): p. 683-93.
2. Rothman, D.L., et al., *In vivo (13) C and (1) H-[(13) C] MRS studies of neuroenergetics and neurotransmitter cycling, applications to neurological and psychiatric disease and brain cancer.* NMR Biomed, 2019. **32**(10): p. e4172.
3. Wijnen, J.P., et al., *In vivo 13C magnetic resonance spectroscopy of a human brain tumor after application of 13C-1-enriched glucose.* Magn Reson Imaging, 2010. **28**(5): p. 690-7.
4. Brender, J.R., et al., *Dynamic Imaging of Glucose and Lactate Metabolism by (13)C-MRS without Hyperpolarization.* Sci Rep, 2019. **9**(1): p. 3410.
5. Kurhanewicz, J., et al., *Hyperpolarized (13)C MRI: Path to Clinical Translation in Oncology.* Neoplasia, 2019. **21**(1): p. 1-16.
6. Rodrigues, T.B., et al., *Magnetic resonance imaging of tumor glycolysis using hyperpolarized 13C-labeled glucose.* Nat Med, 2014. **20**(1): p. 93-7.
7. van Zijl, P.C. and N.N. Yadav, *Chemical exchange saturation transfer (CEST): what is in a name and what isn't?* Magn Reson Med, 2011. **65**(4): p. 927-48.
8. Lu, M., et al., *Quantitative assessment of brain glucose metabolic rates using in vivo deuterium magnetic resonance spectroscopy.* J Cereb Blood Flow Metab, 2017. **37**(11): p. 3518-3530.

9. De Feyter, H.M., et al., *Deuterium metabolic imaging (DMI) for MRI-based 3D mapping of metabolism in vivo.* Sci Adv, 2018. **4**(8): p. eaat7314.
10. De Feyter, H.M. and R.A. de Graaf, *Deuterium metabolic imaging - Back to the future.* J Magn Reson, 2021. **326**: p. 106932.
11. Kreis, F., et al., *Measuring Tumor Glycolytic Flux in Vivo by Using Fast Deuterium MRI.* Radiology, 2020. **294**(2): p. 289-296.
12. Glunde, K., Z.M. Bhujwalla, and S.M. Ronen, *Choline metabolism in malignant transformation.* Nat Rev Cancer, 2011. **11**(12): p. 835-48.
13. Hara, T., *11C-choline and 2-deoxy-2-[18F]fluoro-D-glucose in tumor imaging with positron emission tomography.* Mol Imaging Biol, 2002. **4**(4): p. 267-73.
14. Treglia, G., et al., *The role of positron emission tomography using carbon-11 and fluorine-18 choline in tumors other than prostate cancer: a systematic review.* Ann Nucl Med, 2012. **26**(6): p. 451-61.
15. Kobus, T., et al., *Mapping of prostate cancer by 1H MRSI.* NMR Biomed, 2014. **27**(1): p. 39-52.
16. Peeters, T.H., et al., *3D (31) P MR spectroscopic imaging of the human brain at 3 T with a (31) P receive array: An assessment of (1) H decoupling, T1 relaxation times, (1) H-(31) P nuclear Overhauser effects and NAD().* NMR Biomed, 2021. **34**(5): p. e4169.
17. Esmaeili, M., et al., *IDH1 R132H mutation generates a distinct phospholipid metabolite profile in glioma.* Cancer Res, 2014. **74**(17): p. 4898-907.
18. Vanhamme, L., A. van den Boogaart, and S. Van Huffel, *Improved method for accurate and efficient quantification of MRS data with use of prior knowledge.* J Magn Reson, 1997. **129**(1): p. 35-43.
19. Freeman, J.J., R.L. Choi, and D.J. Jenden, *Plasma choline: its turnover and exchange with brain choline.* J Neurochem, 1975. **24**(4): p. 729-34.
20. Katz-Brull, R., et al., *Choline metabolism in breast cancer; 2H-, 13C- and 31P-NMR studies of cells and tumors.* MAGMA, 1998. **6**(1): p. 44-52.
21. de Graaf, R.A., et al., *On the magnetic field dependence of deuterium metabolic imaging.* NMR Biomed, 2020. **33**(3): p. e4235.
22. Ueland, P.M., *Choline and betaine in health and disease.* J Inherit Metab Dis, 2011. **34**(1): p. 3-15.
23. De Feyter, H.M., Thomas M.A., Ip K.L., Behar K.I., de Graaf R.A. . *Delayed mapping of 2H-labeled choline using Deuterium Metabolic Imaging (DMI) reveals active choline metabolism in rat glioblastoma.* . in *Proceedings of the International Society of Magnetic Resonance in Medicine*. 2021. Virtual.
24. Agut, J., et al., *Dissimilar effects in acute toxicity studies of CDP-choline and choline.* Arzneimittelforschung, 1983. **33**(7A): p. 1016-8.
25. Ip KL, T.M., Khunte A, Behar KL, de Graaf RA, de Feyter HM. *Mapping of exogenous choline uptake in brain tumors in vivo using deuterium metabolic imaging (DMI)*. in *Proceeding of the International Society of Magnetic Resonance in Medicine*. 2020. Virtual
26. Modinger, Y., et al., *Plasma Kinetics of Choline and Choline Metabolites After A Single Dose of SuperbaBoost(TM) Krill Oil or Choline Bitartrate in Healthy Volunteers.* Nutrients, 2019. **11**(10).
27. Buchman, A.L., et al., *Choline pharmacokinetics during intermittent intravenous choline infusion in human subjects.* Clin Pharmacol Ther, 1994. **55**(3): p. 277-83.
28. Friesen-Waldner, L.J., et al., *Hyperpolarized choline as an MR imaging molecular probe: feasibility of in vivo imaging in a rat model.* J Magn Reson Imaging, 2015. **41**(4): p. 917-23.
29. Cudalbu, C., et al., *Feasibility of in vivo 15N MRS detection of hyperpolarized 15N labeled choline in rats.* Phys Chem Chem Phys, 2010. **12**(22): p. 5818-23.
30. Kumar, M., et al., *Magnetic resonance spectroscopy for detection of choline kinase inhibition in the treatment of brain tumors.* Mol Cancer Ther, 2015. **14**(4): p. 899-908.
31. Hamans, B., et al., *Multivoxel (1)H MR spectroscopy is superior to contrast-enhanced MRI for response assessment after anti-angiogenic treatment of orthotopic human glioma xenografts and provides handles for metabolic targeting.* Neuro Oncol, 2013. **15**(12): p. 1615-24.
32. Chiti, A. and M. Picchio, *The rising PET: the increasing use of choline PET/CT in prostate cancer.* Eur J Nucl Med Mol Imaging, 2011. **38**(1): p. 53-4.

33. Lin, C.Y., et al., *Comparing the Staging/Restaging Performance of 68Ga-Labeled Prostate-Specific Membrane Antigen and 18F-Choline PET/CT in Prostate Cancer: A Systematic Review and Meta-analysis.* Clin Nucl Med, 2019. **44**(5): p. 365-376.
34. Gursan A, H.A., Welting D, Klomp D, Prompers JJ *Monitoring liver glucose uptake and metabolism with dynamic 3D deuterium metabolic imaging at 7T*. in *Proceeding of the International Society of Magnetic Resonance in Medicine*. 2021. Virtual.
35. Adebayo A, D.K., Watkins R, Liu SC, Hurd R, Spielman DM. *Deep Learning using synthethic data for signal denoising and spectral fitting in deuterium metabolic imaging*. in *Proceedings of the International Society of Magnetic Resonance in Medicine*. 2021. Virtual.
36. Hesse, F., et al., *Monitoring tumor cell death in murine tumor models using deuterium magnetic resonance spectroscopy and spectroscopic imaging.* Proc Natl Acad Sci U S A, 2021. **118**(12).